

1973

Electrochemical Reduction of Molybdenum(VI) Compounds in Molten Lithium Chloride-Potassium Chloride Eutectic

Branko N. Popov

University of South Carolina - Columbia, popov@engr.sc.edu

H. A. Laitinen

University of Illinois at Urbana

Follow this and additional works at: https://scholarcommons.sc.edu/eche_facpub

 Part of the [Chemical Engineering Commons](#)

Publication Info

Journal of the Electrochemical Society, 1973, pages 1346-1350.

© The Electrochemical Society, Inc. 1973. All rights reserved. Except as provided under U.S. copyright law, this work may not be reproduced, resold, distributed, or modified without the express permission of The Electrochemical Society (ECS). The archival version of this work was published in the *Journal of the Electrochemical Society*.

<http://www.electrochem.org/>

DOI: 10.1149/1.2403259

<http://dx.doi.org/10.1149/1.2403259>

This Article is brought to you by the Chemical Engineering, Department of at Scholar Commons. It has been accepted for inclusion in Faculty Publications by an authorized administrator of Scholar Commons. For more information, please contact digres@mailbox.sc.edu.

T	absolute temperature ($^{\circ}\text{K}$)
U_i	eigenfunctions in series for Φ^t
$U_{i,0}$	value of U_i at the electrode surface
V	electrode potential (V)
V^{ss}	steady-state part of the electrode potential (V)
V^t	transient part of the electrode potential (V)
z	distance from plane of disk (cm)
α_a, α_c	parameters in the kinetic coefficient
δ	Nernst diffusion layer thickness (cm)
$\delta_{m,n}$	Kronecker delta
η	rotational elliptic coordinate
η_s	surface overpotential (V)
κ	conductivity of the solution ($\text{ohm}^{-1}\text{-cm}^{-1}$)
Λ_i	dimensionless eigenvalue
Λ_D	eigenvalue characteristic of diffusion
Φ	potential in the solution (V)
Φ_0	value of Φ at the electrode surface (V)
Φ^{ss}	steady-state part of potential in the solution (V)
Φ^t	transient part of potential in the solution (V)
Φ_0^p	potential in the solution adjacent to the disk corresponding to the primary current distribution (V)
ξ	rotational elliptic coordinate
τ_i	time constants for decay (sec)
θ	dimensionless time for the charging period
θ'	dimensionless time for the decay period
θ_{ch}	dimensionless total period of charging
v_i	constants in the series for V^t (normalized to unity)
Ω	angular frequency of rotation (radians/sec)

REFERENCES

1. S. Glasstone, *J. Chem. Soc.*, **123**, 2926 (1923).
2. A. Hickling, *Trans. Faraday Soc.*, **33**, 1540 (1937).
3. S. Schuldinger and R. E. White, *This Journal*, **97**, 433 (1950).
4. J. D. E. McIntyre and W. F. Peck, Jr., *ibid.*, **117**, 747 (1970).
5. J. Newman, *ibid.*, **113**, 501 (1966).
6. J. Newman, *ibid.*, **113**, 1235 (1966).
7. J. Newman, *ibid.*, **114**, 239 (1967).
8. J. Newman, *ibid.*, **117**, 507 (1970).
9. L. Nanis and W. Kesselman, *ibid.*, **118**, 454 (1971); and *ibid.*, **118**, 1967 (1971).
10. J. Newman, *ibid.*, **118**, 1966 (1971).
11. W. Tiedemann, J. Newman, and D. N. Bennion, *ibid.*, **120**, 256 (1973).
12. B. Miller and M. I. Bellavance, *ibid.*, **120**, 42 (1973).
13. J. Newman, *Intern. J. Heat Mass Transfer*, **10**, 983 (1967).
14. W. R. Parrish and J. Newman, *This Journal*, **116**, 169 (1969).
15. W. R. Parrish and J. Newman, *ibid.*, **117**, 43 (1970).
16. J. Newman, *J. Phys. Chem.*, **73**, 1843 (1969).
17. J. Newman, *This Journal*, **117**, 198 (1970).
18. D. C. Grahame, *Chem. Rev.*, **41**, 441 (1947).
19. E. Levart and D. Schuhmann, *J. Electroanal. Chem.*, **24**, 41 (1970).
20. A. M. Johnson and J. Newman, *This Journal*, **118**, 510 (1971).
21. J. Newman, "Electrochemical Systems," p. 58, Prentice-Hall, Inc., Englewood Cliffs, N. J. (1973).
22. E. Mattsson and J. O'M. Bockris, *Trans. Faraday Soc.*, **55**, 1586 (1959).
23. D.-T. Chin, *This Journal*, **118**, 1434 (1971).
24. R. Parsons, *Advan. Electrochem. Electrochem. Eng.*, **1**, 1 (1961).
25. K. Nisancioğlu and J. Newman, *This Journal*, **120**, 1356 (1973).
26. J. R. Selman, Ph.D. Thesis (UCRL-20557), University of California, Berkeley, June, 1971.
27. L. Nanis and I. Klein, *This Journal*, **119**, 1683 (1972).

Electrochemical Reduction of Molybdenum(VI) Compounds in Molten Lithium Chloride-Potassium Chloride Eutectic

B. N. Popov

Faculty of Technology and Metallurgy, University Kiril and Metodij, Skopje, 91000, Yugoslavia

and H. A. Laitinen*

Roger Adams Laboratory, School of Chemical Sciences, University of Illinois, Urbana, Illinois 61801

ABSTRACT

Molybdenum(VI) oxide reacts with molten LiCl-KCl eutectic at 450 $^{\circ}$ to form MoO_2Cl_2 , which probably is present as an anion $\text{MoO}_2\text{Cl}_4^-$, and pyromolybdate, $\text{Mo}_2\text{O}_7^{2-}$. Both of these species are electrochemically reduced to MoO_2 , which can be reoxidized to MoO_2Cl_2 by current reversal. A second reduction step, observed whether MoO_3 or $\text{Mo}_2\text{O}_7^{2-}$ is added to the melt, can be attributed to the reduction of MoO_4^{2-} , formed as a secondary reaction product in the first step. The reduction of molybdate proceeds in two steps, the first at -0.85V and the second at -1.75V vs. the 1M Pt(II)/Pt reference electrode. The first step shows an abnormally short transition time, attributable to a slow equilibrium. The second step corresponds to a diffusion-controlled reduction with $n = 0.5$, yielding a product of the empirical formula $\text{Li}_5\text{Mo}_2\text{O}_8$.

The literature contains very little fundamental information on the behavior of molybdenum compounds in molten systems. Stavenhagen and Engels (1) described a sodium molybdenum bronze in the form of a dark bluish-grayish powder formed by electrolytic reduction of fused sodium molybdate. Cannery (2) reported the preparation of lithium, sodium, and potassium molybdenum bronzes using the same method. However, the next year Burgers and van Liempt (3) showed that the bronzes mentioned by Cannery were

mixtures consisting of molybdenum(IV) oxide and molybdenum blue. According to Magneli, only molybdenum oxides were obtained by Hagg in similar experiments (4, 5). Wold, Kunmann, Arnot, and Ferretti (6) prepared pure MoO_2 crystals by electrolytic reduction of MoO_3 - Na_2MoO_4 mixtures at 675 $^{\circ}\text{C}$. In addition, both sodium molybdenum bronze and potassium molybdenum bronze crystals were grown from molybdenum(IV) oxide-alkali molybdate melts under carefully controlled conditions. Senderoff and Brenner (7, 8) have investigated the reduction of molybdate dissolved in molten alkali halides. They found that the bulk of the reaction product was dispersed throughout

* Electrochemical Society Active Member.

Key words: molybdenum, molybdenum(VI) oxide, molybdenum oxychloride, lithium pyromolybdate, lithium molybdate, molten salts, electrochemistry.

the melt as a black, water insoluble powder containing about 77% molybdenum, corresponding to MoO_2 (75% Mo).

The present investigation was undertaken in order to study the reduction of molybdenum(VI) compounds and to characterize any reduction products observed. It was also considered possible that some aspects of molybdenum chemistry and interactions between molybdenum(VI) compounds and chloride melt could be deduced.

Experimental

Apparatus.—The instrumentation and equipment used in this study have been previously described (9-11).

Electrodes.—Platinum microelectrodes for voltammetry were prepared from 26B and S gauge platinum wire as described earlier (10). Indicator electrodes for chronopotentiometric measurements were made by sealing 26 gauge platinum wire into Pyrex glass and then spot welding a piece of 0.5 cm^2 platinum foil to the end of the wire extending from the platinum glass seal. The cathodes used for the preparation of the electrode deposits were constructed from 52-mesh platinum gauze. The counterelectrode was a $\frac{1}{8}$ -in. diameter graphite rod. All potentials are referred to the 1M Pt(II)/Pt reference electrode. Details on the generation and use of this reference electrode in LiCl-KCl have been described previously (11, 12).

Chemicals.—All chemicals used in this study were reagent grade. Those chemicals containing water of hydration were vacuum dried at 110°C before being added to the melt.

The LiCl-KCl eutectic was obtained from Anderson Physics Laboratories, Inc., Urbana, Illinois. The method of purification has been described (11). All experiments in the melt were carried out at 450°C unless otherwise noted.

Solid chemicals were added to the melt by means of a small glass spoon. A blanket of argon was kept over the melt at all times to exclude oxygen and water vapor. The purification train used in purifying the argon has been described (13).

Techniques for preparation and analysis of electrode deposits.—Before their insertion in the melt solution, the gauze electrodes were cleaned in boiling, concentrated HNO_3 , rinsed with distilled water, and dried at 130°C for 20 hr. After the material had been deposited on the electrode, the electrode was allowed to cool, washed with deionized water, and dried at 120°C . The deposits were then dissolved in 5 ml of concentrated nitric acid by heating on a hot plate. The molybdenum content of the deposit was determined by addition of an excess of Pb^{2+} which was back-titrated with EDTA using xylenol orange as the indicator. The total molybdenum was also obtained by amperometric titration with lead, a procedure developed by Aylward (14). The amount of reduced molybdenum in the sample was determined by the method developed by Bourret (15). Lithium was quantitatively determined by flame photometry. Chloride was determined by the Volhard method.

Results and Discussion

MoO_3 -LiCl-KCl system.—Preliminary steady-state voltammetric experiments (Fig. 1) showed that MoO_3 exhibits two reduction waves in LiCl-KCl at 450° . The half-wave potentials are approximately -0.3 and -1.75V . The voltammetric curves were not highly reproducible because of the formation of an insoluble product which rapidly increases the surface area of the electrode. Upon prolonged electrolysis at the limiting plateau, a brown-violet film formed on the electrode, and the current increased with time. Chronopotentiometric experiments with proper choice of concentration and current density circumvented the difficulty due to film formation. Two transitions, at -0.35 and -1.75V , respectively, were observed, in agreement with the voltammetric observations. The Sand equation was checked for the first reduction step

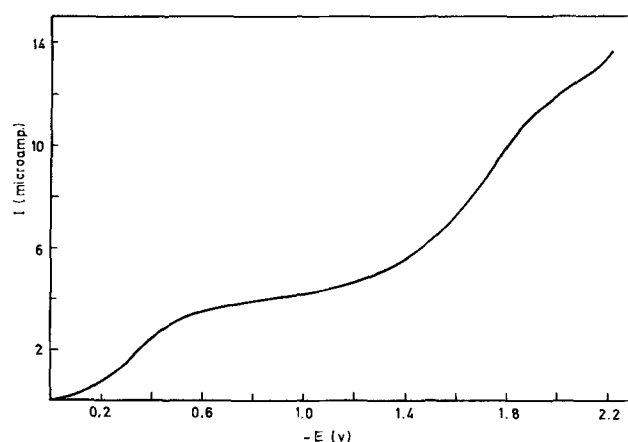


Fig. 1. Current-voltage curve for the reduction of MoO_3 . Electrode area = $2.2 \cdot 10^{-3} \text{ cm}^2$; $\text{MoO}_3 = 3.63 \cdot 10^{-3} \text{ M}$.

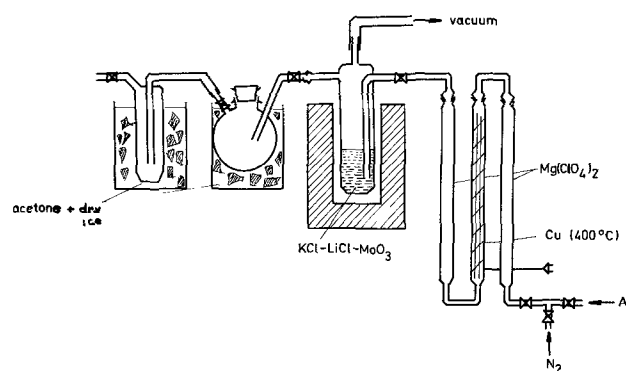


Fig. 2. Apparatus used to study acid-base reaction of MoO_3 and chloride melt.

using four to six current densities at three different MoO_3 concentrations (Table I). Constancy of the quantity $I_{T^{1/2}}/C$ indicated diffusion-controlled reaction. However, it was observed during the measurements that a volatile product was slowly evaporating from the melt. Therefore, owing to the uncertain concentration it was not possible to calculate a valid diffusion coefficient from the data.

To establish the nature of the volatile product, the apparatus shown in Fig. 2 was used. Previously dried MoO_3 was added to the melt, air was excluded, and the volatile product was displaced by inert gas into a weighed trap cooled with acetone and dry ice. The product was yellow in color, very volatile, and soluble in water. Analysis for Mo and Cl^- by the methods described above showed that the sample weight could be completely accounted for in terms of the compound MoO_2Cl_2 . To determine the product formed from the

Table I. Chronopotentiometric data for the first reduction step of MoO_3

C_{MoO_3} (M)	I (mA)	$I_{T^{1/2}}$ (A-sec ^{1/2})	$I_{T^{1/2}}/C$ (A-sec ^{1/2} cm ³ mol ⁻¹)
$3.63 \cdot 10^{-3}$	1.540	$0.784 \cdot 10^{-3}$	210
	1.050	$0.715 \cdot 10^{-3}$	197
	0.550	$0.671 \cdot 10^{-3}$	185
	0.680	$0.664 \cdot 10^{-3}$	183
	0.596	$0.660 \cdot 10^{-3}$	183
	0.630	$0.680 \cdot 10^{-3}$	187
		Avg $0.679 \cdot 10^{-3}$	Avg 187
$9.84 \cdot 10^{-3}$	2.500	$1.802 \cdot 10^{-3}$	183
	2.000	$1.780 \cdot 10^{-3}$	181
	1.670	$1.734 \cdot 10^{-3}$	176
	1.430	$1.770 \cdot 10^{-3}$	181
		Avg $1.770 \cdot 10^{-3}$	Avg 181
$2.3 \cdot 10^{-2}$	10.000	$4.250 \cdot 10^{-3}$	185
	6.870	$4.200 \cdot 10^{-3}$	183
	5.550	$4.350 \cdot 10^{-3}$	189
	4.540	$4.140 \cdot 10^{-3}$	180
		Avg $4.230 \cdot 10^{-3}$	Avg 184

reaction of the oxide ion, the melt was extracted from the product with ethanol and acetone to yield $\text{Li}_2\text{Mo}_2\text{O}_7$, which accounted completely for the sample weight. Accordingly the reaction between MoO_3 and the melt can be written



A phase diagram study of MoO_3 and Li_2MoO_4 was carried out to verify further the existence of $\text{Li}_2\text{Mo}_2\text{O}_7$. Phase transition temperatures were determined for eight samples ranging in composition from 42 to 55 m/o (mole per cent) MoO_3 . The experiments were done by the visual polythermal method in which the temperature of the first crystals was measured by a Pt-Rh thermocouple. From Table II it is evident that a local maximum exists for the molar ratio $\text{MoO}_3/\text{Li}_2\text{MoO}_4 = 1$, implying the formation of a solid compound $\text{Li}_2\text{Mo}_2\text{O}_7$. An x-ray powder pattern of the 1:1 sample is described in Table III. No lines for MoO_3 or Li_2MoO_4 were found in the diffraction pattern, thus precluding the possibility that the material is a mixture of MoO_3 and Li_2MoO_4 .

To determine whether the acid-base reaction occurs completely before the electrolysis experiments, the data of Table I were examined for a chemical reaction preceding charge transfer by plotting $I_0\tau^{1/2}/C$ vs. I_0 and I_0/C . The plots showed no discernible downward slope, but only a scatter that could be attributed to uncertainties in concentration owing to volatility of the oxychloride, and perhaps to variation in electrode area with the formation of solid deposit.

Plots of E vs. $\log(\tau^{1/2} - t^{1/2})$ were linear as shown in Fig. 3. This function would be expected to yield linear plots either for a totally irreversible charge transfer process or for a reversible process with the formation of a solid product of constant activity. Current reversal chronopotentiometry showed an anodic transition upon reversal of the current at the inflection point (Fig. 4): ratios of the coulombs of charge in the forward to backward electrolysis varied between 0.985 and 1.025, indicating the quantitative formation of a solid product that can be reoxidized. If the slope of the log plot is equated to $2.3 RT/\alpha n_a F$, we calculate

Table II. Melting points of MoO_3 - Li_2MoO_4 system

Mole per cent MoO_3	Mole per cent Li_2MoO_4	Melting point, °C
42	58	550
45	55	520
48	52	495
49	51	526
50	50	534
51	49	515
53	47	535
55	45	555

Table III. X-ray powder diffraction pattern of $\text{Li}_2\text{Mo}_2\text{O}_7$

d (Å)	I/I_0
6.4241	10
5.3679	10
4.1385	30
3.7824	10
3.6820	10
3.5199	80
2.9809	50
2.9780	50
2.8823	10
2.8331	10
2.7136	50
2.5074	10
2.3659	10
2.1917	100
2.1396	50
2.0064	60
1.9012	80
1.8398	5
1.8294	5
1.8030	5
1.7697	5
1.7323	5
1.6937	70
1.6161	10
1.5900	20
1.5522	90
1.5043	40

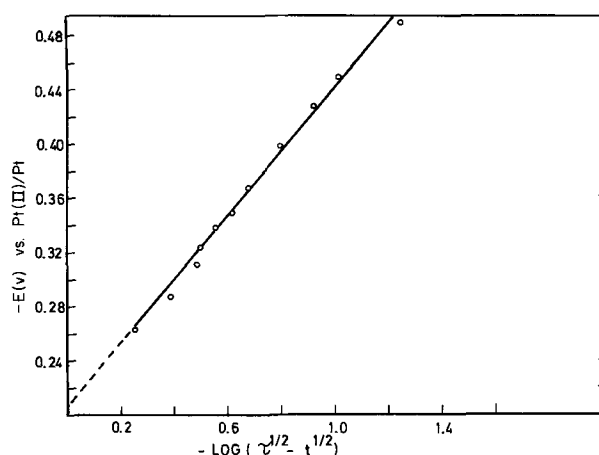


Fig. 3. Potential-time curve for the first reduction step of MoO_3 .

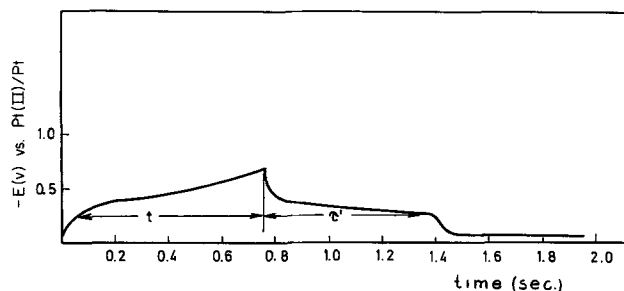


Fig. 4. Typical reverse current chronopotentiogram for the first reduction step of MoO_3 . $I_f = I_r = 2.0 \text{ mA/cm}^2$.

$\alpha n_a = 0.56$ rather than 2 for a reversible process. Neglecting the back-reaction, the value of $k_{f,h}$ at -0.208V , the starting potential, is calculated to be $3.18 \times 10^{-3} \text{ cm-sec}^{-1}$.

Analysis of the reduction products of MoO_3 .—Samples of the first reduction product, prepared coulometrically from 0.35M MoO_3 solution using a platinum gauze cathode, in the form of a homogeneous, brown-violet solid, were boiled in distilled water to remove chlorides and soluble molybdates and dried at 130° . Analysis revealed only MoO_2 , and the x-ray powder pattern agreed in d-spacings and approximate relative densities with the ASTM files for MoO_2 .

Attempts were also made to prepare the second reduction product, by holding the potential of the working electrode at -1.75V . A product showing x-ray lines of MoO_2 , plus several weak lines, and containing Li but not K was formed, corresponding to a mixture of the first and second reduction products. The composition could not be completely accounted for in terms of MoO_2 and Li_2O or Mo_2O_5 and Li_2O . It is possible that the second reduction product is partially soluble in the melt.

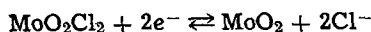
MoO_2Cl_2 -LiCl-KCl-system.—The solubility of MoO_2Cl_2 in the melt was determined at three temperatures, 400° , 450° , and 500° , by saturating an argon gas stream with the vapor and bubbling the dilute stream (heated to 120° to avoid crystallization from the vapor) through the melt for at least 2 hr, and analyzing the melt for molybdenum. The solubility was found to be 2.60 ± 0.12 , 2.75 ± 0.14 , and $2.78 \pm 0.09 \times 10^{-5}$ moles $\text{MoO}_2\text{Cl}_2/\text{cm}^3$ at the three temperatures. The relatively high solubility and low vapor pressure over the melt indicates a strong interaction between MoO_2Cl_2 , probably to form an anion $\text{MoO}_2\text{Cl}_4^-$ with the chloride ion of the melt.

Chronopotentiometry indicated a single wave, occurring at a potential of -0.35V , in agreement with the postulated interaction between MoO_3 and melt. From the value of $I_0\tau^{1/2}/C = 560 \pm 10 \text{ A-sec}^{1/2} \text{ cm mol}^{-1}$, $n = 2$, the diffusion coefficient was calculated to be $1.08 \times 10^{-5} \text{ cm}^2/\text{sec}$.

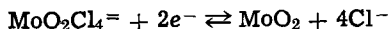
Table IV. Chronopotentiometric data for the first reduction step of $\text{Li}_2\text{Mo}_2\text{O}_7$

$C_{\text{Mo}_2\text{O}_7^{2-}}$ (millimolar)	I_0 (mA)	$I_0\tau^{1/2}$ (mA-sec ^{1/2} /cm ²)	$I_0\tau^{1/2}/C$ (A-sec ^{1/2} /cm ² mole ⁻¹)
3.48	1.60	1.92	552
	2.00	1.82	524
	2.44	1.81	520
	3.00	1.77	509
			Avg 526
10.80	6.00	4.97	460
	7.00	4.85	449
	7.50	4.77	442
	8.00	4.55	421
			Avg 443
21.23	6.00	8.15	383
	8.00	7.84	369
	9.00	7.74	364
	10.00	7.80	366
			Avg 371
95.40	28.00	33.05	348
	30.00	31.20	327
	34.00	31.28	331
	36.00	30.96	324
			Avg 332

Constant current electrolysis carried out at potentials never more negative than -0.35V , of a solution of MoO_2Cl_2 prepared by bubbling the vapor through the melt for 2 hr produced a brown-violet deposit. Comparison of the micromoles of molybdenum with the microfaradays of current consumed indicated a consumption of two electrons per molybdenum atom. The x-ray powder pattern agreed with that of the first reduction product of MoO_3 and with the ASTM pattern of MoO_2 . The electrode reaction at -0.35V can thus be described as

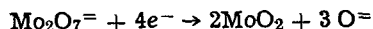


or

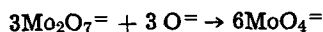


$\text{Li}_2\text{Mo}_2\text{O}_7$ -LiCl-KCl system.—The chronopotentiometric behavior of $\text{Li}_2\text{Mo}_2\text{O}_7$ was found to be quite similar to that of MoO_3 . Two waves were observed, one at -0.44V and the other at approximately -1.75V . The transition time data for the first reduction process (Table IV) were somewhat scattered, showing a trend to decrease with concentration and with increasing current density. When both MoO_3 (3.55 mM) and $\text{Li}_2\text{Mo}_2\text{O}_7$ (2.15 mM) were present, two waves were once again observed, one at -0.37V and the other at -1.75V . It is concluded that the first wave of MoO_3 is actually the sum of the first waves of MoO_2Cl_2 and $\text{Mo}_2\text{O}_7^{2-}$.

The first reduction product of $\text{Li}_2\text{Mo}_2\text{O}_7$ was characterized as before, and identified as MoO_2 . Accordingly, the first reduction process can be written

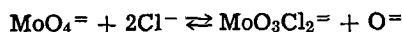


with a following acid-base reaction, no doubt

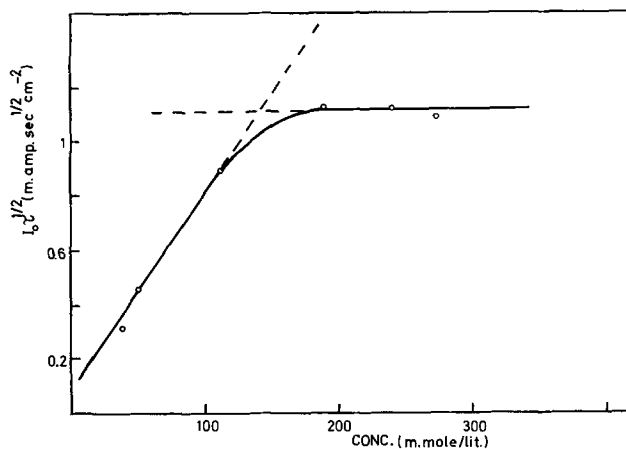


The complexity of this process presumably accounts for the lack of diffusion control in the over-all process.

MoO_4^{2-} -LiCl-KCl system.—Chronopotentiograms were recorded over a concentration range of $8.03 \times 10^{-3}\text{M}$ to 0.2725M Li_2MoO_4 . At current densities below 2 mA/cm^2 , two waves were discerned, one at -0.85V and the other at -1.75V . The first wave increased with concentration until the concentration reached $1.12 \times 10^{-2}\text{M}$, and leveled off at higher concentrations (Fig. 5). The slope of the plot at low concentrations yielded $I_0\tau^{1/2}/C = 9.87 \pm 0.6\text{ A-sec}^{1/2}/\text{cm}^2\text{ mole}^{-1}$, corresponding to $nD^{1/2} = 1.45 \times 10^{-4}\text{ cm-sec}^{-1/2}$. Such an abnormally low transition time constant suggests an equilibrium such as



in which MoO_3Cl_2 exists as a minority component responsible for the first reduction step. If such an equilibrium exists, it must be relatively slow, because $I_0\tau^{1/2}$ was not found to decrease with increasing cur-

Fig. 5. Variation of $I_0\tau^{1/2}$ with Li_2MoO_4 concentration for the first reduction step.

rent density as would be expected for a prior chemical step with appreciable interconversion during the time of electrolysis.

With a molybdate concentration of $5.35 \times 10^{-2}\text{M}$ and with a current density of 16 mA/cm^2 only the second transition was observed. The Sand equation was tested for four to five current densities at five different molybdate concentrations (Table V). The average value of $I_0\tau^{1/2}/C$ calculated from these data is $174 \pm 6\text{ A-sec}^{1/2}/\text{cm}^2\text{ mole}^{-1}$, corresponding to $D = 1.64 \times 10^{-5}\text{ cm-sec}^{-1}$ at 450° , taking $n = 0.5$ from the analytical data given below.

Attempts to prepare the first reduction product by constant current electrolysis were unsuccessful. Using 0.85M Li_2MoO_4 , even with current densities lower than $100\text{ }\mu\text{A/cm}^2$, the electrode potential rapidly rose beyond that corresponding to the first reduction step. Using current densities of $100\text{ }\mu\text{A}$, 5 mA , and 10 mA/cm^2 , deposits were prepared by electrolyzing at -1.18 to -1.2V , at -1.5V , and at -1.75V , respectively. Examination of the cathodes showed only one type of solid product, an adherent dark brown-black solid with a metallic luster. The samples were washed with distilled water, dried at 130° , and analyzed for Li and Mo with the results given in Table VI. The deposit was found to contain an average of 54.0% Mo and 9.85% Li but no K or Cl. The ratio Li/Mo is 2.52 . No appreciable trend of composition with current density was observed. If it is assumed that the deposit contains only Li, Mo, and O, the empirical formula $\text{Li}_{2.49}\text{MoO}_{3.96}$ is obtained indicating an average oxidation state of 5.5 for molybdenum.

Additional preparations produced at -1.75V were analyzed for oxidation state, with the results listed in Table VII. The sum of Li_2O , Mo_2O_5 , and MoO_3 is very close to 100% , confirming the absence of K and Cl, and indicating once more that the product is $\text{Li}_{2.5}\text{MoO}_4$ or $\text{Li}_5\text{Mo}_2\text{O}_8$. To ascertain whether the product is a single compound or a mixture, an x-ray powder pattern was obtained for the products prepared at -1.2 , -1.5 , and -1.75V . The d spacing along with relative intensities are given in Table VIII. No lines for LiCl or Li_2MoO_4 were found in the diffraction pattern. The diffraction data do not correspond with any known molybdenum compound listed in the ASTM files or with other deposits obtained by reduction of Mo(VI) compounds.

Table V. Chronopotentiometric data for the second reduction step of lithium molybdate

Molybdate conc. (millimolar)	$I_0\tau^{1/2}$ (mA-sec ^{1/2} /cm ²)	Range of I_0 (mA/cm ²)
8.03	1.29 ± 0.08	2.5-4.0
20.80	3.46 ± 0.06	6.0-10.0
53.50	9.72 ± 0.09	24.0-20.0
110.02	20.04 ± 0.18	24.0-44.0
178.05	31.00 ± 0.90	28.0-34.0

Table VI. Typical analysis of Li_2MoO_4 deposit prepared at constant current

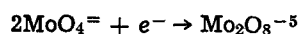
Sample	A	B	C	D	E	F
Current density, mA/cm ²	5	5	5	10	10	10
Sample weight, mg	73.5	129.9	112.5	150.6	148.2	134.5
Li, mg found	7.17	12.7	11.0	15.2	14.7	13.2
Per cent weight Li	9.7	9.8	9.8	10.1	9.9	9.9
Mo, mg found	39.6	70.6	61.1	81.2	80.23	72.2
Per cent weight Mo	53.9	54.4	54.1	53.8	54.0	53.6
Per cent weight O = to 100%	36.3	35.8	36.1	36.1	36.1	36.5
Li found, μmoles	1035	1830	1585	2200	2120	1910
Mo found, μmoles	412	736	636	846	835	753
O calculated, μmoles	1670	2920	2520	3380	3320	3065
Empirical formula	$\text{Li}_{2.51}\text{MoO}_{3.95}$	$\text{Li}_{2.49}\text{MoO}_{3.96}$	$\text{Li}_{2.49}\text{MoO}_{3.95}$	$\text{Li}_{2.56}\text{MoO}_{3.99}$	$\text{Li}_{2.55}\text{MoO}_{3.98}$	$\text{Li}_{2.54}\text{MoO}_{4.07}$

Table VII. Determination of the empirical formula of Li_2MoO_4 deposit prepared at constant potential

Sample	A	B	C	D
Milliliters 0.05N $\text{Na}_2\text{S}_2\text{O}_8$	6.29	7.42	8.54	9.40
Milligrams NaIO_3 calculated	25.9	29.8	35.2	38.7
Milligram total Mo calculated	50.7	60.7	67.7	78.2
Average valence of Mo	5.50	5.51	5.49	5.52
Micromoles Li	1320	1600	1730	2010
Milligrams Li_2O	19.8	23.8	25.9	30.1
Total Mo, mg	50.7	60.7	67.5	78.2
Micromoles Mo	528	632	702	815
Milligrams Mo(V)	25.0	29.8	34.2	37.8
Milligrams Mo_2O_5	35.6	42.2	48.5	53.6
Milligrams Mo(VI)	25.7	31.0	33.3	40.4
Milligrams MoO_3	38.4	46.2	50.0	60.6
Total mg found	93.8	112.3	124.3	144.4
Sample weight, mg	92.6	113.5	123.1	143.3
Per cent weight found	101.9	99.2	101.0	100.5
Empirical formula	$\text{Li}_{2.50}\text{MoO}_{4.00}$	$\text{Li}_{2.52}\text{MoO}_{4.03}$	$\text{Li}_{2.48}\text{MoO}_{3.98}$	$\text{Li}_{2.47}\text{MoO}_{3.99}$

To study the stability of the product, one sample was heated at 300° under vacuum. No change in diffraction pattern was observed. The deposit was further boiled in distilled water 3 hr and dried at 200°. The boiled product exhibited a different x-ray pattern as shown in Table IX. The analytical data indicated Li/Mo to be 4.43/2 and the sum of the weight percentages of $\text{Li}_2\text{O} + \text{MoO}_3$ to be 97.66, indicating the presence of water in the sample or partial oxidation of Mo_2O_5 .

The electrode reaction of molybdate can be written



The mechanism of this reaction is unclear. There is no evidence for dimerization of molybdate prior to reduction, and the diffusion coefficient is consistent

with our expectation for a monomer. The simplest mechanism would be the formation of the anion MoO_4^{3-} , with the incorporation of equimolar amounts of MoO_4^{2-} with lithium ions to form the crystalline compound $\text{Li}_5\text{Mo}_2\text{O}_8$.

Acknowledgment

One of the authors (B. N. P.) is indebted to the University of Illinois for the support in the form of research assistantship. Financial support of this research was provided by the United States Army Research Office-Durham and by the Center for Application of Radioisotopes in Industry, Skopje, Yugoslavia.

Manuscript submitted March 30, 1973; revised manuscript received May 18, 1973.

Any discussion of this paper will appear in a Discussion Section to be published in the June 1974 JOURNAL.

Table VIII. X-ray powder diffraction pattern of $\text{Li}_5\text{Mo}_2\text{O}_8$

d (Å)	I/I ₀
4.9130	60
2.4661	60
2.3659	20
2.0740	100
1.9125	20
1.4912	40
1.4443	40
1.3882	40

Table IX. X-ray powder diffraction pattern of boiled deposit

(Å)	I/I ₀
3.6302	60
3.2785	30
2.9568	10
2.6727	100
2.5510	10
2.2046	30
2.0279	30
1.8845	10
1.8345	10
1.7172	20
1.6752	20

REFERENCES

1. A. Stavenhagen and E. Engels, *Ber.*, **28**, 2281 (1895).
2. C. Cannery, *Gazz. Chim. Ital.*, **60**, 113 (1930).
3. W. G. Burgers and J. A. M. Van Liempt, *Z. Anorg. Allgem. Chem.*, **302**, 325 (1931).
4. A. Magnéli, *N. Acta Reg., Sc. Upsaliensis*, **14**, No. 816 (1939).
5. G. Hagg, *Z. Physik. Chem.*, **B29**, 192 (1935).
6. A. Wold, W. Kunmann, R. J. Arnott, and A. Ferretti, *Inorganic Chem.*, **3**, 545 (1964).
7. S. Senderoff and A. Brenner, *This Journal*, **101**, 16 (1954).
8. S. Senderoff and A. Brenner, *ibid.*, **101**, 31 (1954).
9. H. A. Laitinen and J. H. Propp, *Anal. Chem.*, **38**, 644 (1969).
10. H. A. Laitinen and B. N. Popov, *This Journal*, **117**, 482 (1970).
11. H. A. Laitinen and K. W. Hanck, *ibid.*, **118**, 1123 (1971).
12. H. A. Laitinen and K. R. Lucas, *ibid.*, **12**, 553 (1966).
13. H. A. Laitinen and D. R. Rhodes, *ibid.*, **10**, 413 (1962).
14. G. H. Aylward, *Anal. Chim. Acta*, **14**, 386 (1956).
15. P. Bourret, J. M. Lecure, and K. Weis, *Chim. Anal. (Paris)*, **52**, (1) 48 (1970).